zolium chloride and aluminum chloride at ambient temperature. The plating and stripping rates are high for an ambient-temperature, nonaqueous system, and the quantity of aluminum is energetically useful for battery applications. The aluminum electrode shows high cycling efficiency which does not deteriorate as the rate is increased. The chloraluminate melt is stable and·does not decompose on cycling. The relatively high positive potential of aluminum and the requirement of large quantities of melt to accommodate composition changes limit its application as a practical, high energy secondary battery.

Manuscript submitted Sept. 20, 1984.

REFERENCES

1. R. Gale and R. Osteryoung, *Inorg. Chem.*, **18**, 1603 (1979).
2. J. S. Wilkes, J. A. Levisky, R. A. Wilson, and C. L.
   Hussey, *ibid.*, **21**, 1263 (1982).
3. J. S. Wilkes and J. J. Auborn, Abstract 242, p. 381, The Electrochemical Society Extended Abstracts, Vol. 83-2, Washington, DC, Oct. 9-14, 1983.
4. A. A. Fannin, L. King, J. A. Levisky, and J. S. Wilkes, *J. Phys. Chem.*, **88**, 2609 (1984).
5. A. A. Fannin, D. A. Floreani, L. A. King, J. S. Landers, B. J. Piersma, D. J. Stech, R. L. Vaughn, J. L. Williams, and J. S. Wilkes, *ibid.*, **88**, 2614 (1984).
6. J. S. Wilkes, Unpublished data.
7. K. M. Abraham and S. B. Brummer, in "Lithium Batteries," J. P. Gabano, Editor, p. 379, Academic Press, London (1983).
8. K. T. Ciemiecki and J. J. Auborn, in "Lithium Batteries," A. N. Day, Editor, p. 363, The Electrochemical Society Softbound Proceedings Series, Pennington, NJ (1984).
9. B. J. Piersma and J. S. Wilkes, FJSRL-TR-82-0004, ADA122840, September 1982.
10. C. J. Dymek, Jr., J. L. Williams, D. J. Groeger, and J. J. Auborn, *This Journal*, In press.
11. J. J. Auborn and C. J. Dymek, Jr., Unpublished data.

Two-Phase Mass Transfer in Channel Electrolyzers with Gas-Liquid Flow

Demetre J. Economou** and Richard C. Alkire*

Department of Chemical Engineering, University of Illinois, Urbana, Illinois 61801

ABSTRACT

The electrochemical limiting current method was employed to study the mass transfer to a solid electrode in cocurrent gas-liquid flow through a vertical parallel-plate electrolyzer. Three systems were investigated: aqueous ferricyanide, aqueous ferricyanide containing a dispersion of nitrogen bubbles, and aqueous electrolyte containing a dispersion of oxygen bubbles in equilibrium with the liquid phase. The total mass-transfer rate was found to be the sum of three contributions: (i) the one-phase convective rate associated with the liquid as if it were flowing alone through the cell; (ii) the enhancement of mass transfer owing to disruption of the mass-transfer boundary layer, even by bubbles containing inert gas; and (iii) the further enhancement owing to penetration of the mass-transfer boundary layer by bubbles containing reactive gas. A series of controlled experiments was conducted to determine the dependence of these enhancement mechanisms upon operating variables such as gas and liquid flow rates, bubble size, and electrode material. It was found that, although the conversion per pass through the cell was negligible, a sevenfold increase in the mass transfer, as compared to one-phase flow with the same liquid velocity, was obtained with a reactive gas void fraction as low as 10%.

Because electrochemical reactions are heterogeneous, industrial processes require high mass-transfer rates to minimize capital investment and, simultaneously, large electrode surface areas to achieve high production rates. Strategies for obtaining high mass-transfer rates include increasing the concentration driving force, as by improving reactant solubility, and augmenting the mass-transfer coefficient, as by vigorous stirring. In the case of parallel-plate electrolyzers, such strategies include operation in turbulent flow, evolution of gas which causes vigorous agitation at the electrode surface, use of turbulence promoters, and judicious employment of two-phase flow phenomena. In particular, two-phase processes can meet competing requirements for high mass-transfer rates while maintaining low pressure drop through the cell and also high loading of reactive species, which may be sparingly soluble in the continuous conductive phase.·

In the present work, a study was undertaken of the mass transfer to a solid electrode in upward, cocurrent flow of a gas-liquid mixture introduced into a channel electrolyzer (1). In such flows, the presence of gas bubbles results in an enhancement of the mass-transfer rates over those which would be obtained with one-phase liquid flow alone. This enhancement may be attributed to two effects. First, there is the physical disruption of the mass-transfer boundary layer, caused by the stirring action of dispersed gas bubbles, even by electrochemically inert gases. This type of enhancement will be referred to

as the "disturbance mechanism." Second, when the gas is electrochemically reactive, there is a further enhancement by extraction of reactive material from those bubbles which penetrate to regions very close to the electrode surface. This type of enhancement arises from the replenishment of reactants in depleted regions of the mass-transfer boundary layer and will be referred to as the "extraction mechanism." The purpose of this work was to conduct a series of controlled experiments to determine the dependence of these enhancement mechanisms upon operating variables.

Analysis of electrochemical mass-transfer limiting current data can provide information on the individual elements of the overall mass-transfer mechanism. For example, Lu and Alkire (2) studied mass transfer to solid electrodes in the presence of a second dispersed liquid phase and found that addition of individual coefficients could be used to predict the overall rate. With nomenclature applicable to gas-liquid systems, the concept would be

$$i_t = i_o + i_d + i_e = n\mathbf{F} \left(k_o c_{bl} + k_d c_{bl} + k_e c_{bG} \right) \qquad [1]$$

The first term within the parentheses represents the mass-transfer rate owing to the one-phase convective flow. The second gives the enhancement by the disturbance mechanism, and the third gives the further enhancement by the extraction mechanism. While k_o may be calculated from first principles for simple flow configurations, there is no such theory for prediction of k_d and k_e.

The different concepts for enhancing mass transfer in industrial or large-scale cells have been reviewed by Houghton and Kuhn (3). A detailed description of mass transfer in parallel-plate electrochemical reactors is available (4, 33). Transport processes to the walls of narrow gap channels have been studied by Acosta et al. (34). Mass (or heat) transfer from a two-phase mixture to a heterogeneous boundary such as pipe wall or electrode surface has been actively investigated. Postlethwaite and Holdner (5) obtained an enhancement of the mass transfer of dissolved oxygen to a pipeline wall of up to 100% when sand particles were suspended in the flowing liquid. Dworak et al. (6, 7) observed weakly enhanced mass transfer by dispersing CCl_4 in aqueous ferricyanide flowing past a horizontal Ni electrode. Furthermore, by using a microelectrode and the reactant in the dispersed second phase only, they found that under the experimental conditions used the dispersed droplets did not wet the electrode surface.

However, Lu and Alkire (2) found a mass-transfer enhancement of up to 170% by dispersing inert toluene droplets in aqueous ferricyanide in laminar flow past vertical planar electrodes. In the presence of a reactive second phase, it was found that a nonpolar electrode (graphite) gave significantly higher mass-transfer rates when compared to a polar electrode (DSA®), which suggests that wetting occurred. It was further found that for reactants which are sparingly soluble in the aqueous phase, mass transfer could be augmented by orders of magnitude by using a reactive second phase.

Gas-liquid systems have been widely studied owing to their relevance to many chemical engineering operations. The literature on interfacial mass transport, bubble columns (8), and gas-liquid flows in general (9) is voluminous. Heat-transfer studies from the two-phase mixture to the walls of a bubble column have been reported by Mersmann (10), Steiff and Weinspach (11), and Deckwer (12), among others.

From the electrochemical engineering point of view, one may distinguish between two situations involving gas-liquid mixtures: (a) gas evolving electrodes and (b) gas sparging. Gas evolution is commonly found in the electrochemical industry (H_2O electrolysis, chlor-alkali cell, chlorate cell, etc.) and has been reviewed by Vogt (13). As the bubbles form and break away, they stir the solution adjacent to the electrode enhancing mass transport. The case of superimposed external hydrodynamic flow has been considered by Beck (14) and Vogt (15). In particular, Beck proposed an additive mass-transfer model to account for simultaneous gas evolution and fluid flow. The additivity of the mass-transfer coefficients was subsequently verified (16), and the same concept was used to describe mass transfer in two-phase flows (Ref. (2, 17) and Eq. [1]). Gas sparging is an attractive mode of artificial stirring in electrochemical processes (18, 24). For example, open-topped tanks with widely spaced electrodes used in the metal finishing industry are agitated by introducing air at the bottom of the tank. Significant contributions to the field have been made by Ibl and co-workers. Ibl et al. (18) introduced N_2 through porous frits at the bottom of a vertical parallel-plate cell having a sectioned cathode. The mass-transfer coefficient was uniform throughout the electrode surface and the mass-transfer rate increased with increasing gas flow rate, although the rate leveled off at high gas flow rates. Frit pore size and, therefore, bubble size had no effect on mass transfer. The authors noted that mass-transfer coefficients one order of magnitude higher than those in natural convection can be achieved.

In another study, Ibl (19) injected gas through porous frits in the annular space between two concentric cylinders and obtained mass-transfer coefficients of up to 5.2 10^{-3} cm/s. The influence on the working electrode of gas bubbles generated by the counterelectrode in a parallel-plate cell was investigated by Sigrist et al. (20). The study was conducted with and without superimposed electrolyte flow. It was found that, irrespective of the mode of

operation, the mass-transfer coefficient was dependent on the gas void fraction alone. The experimental data were correlated with an equation resembling that of turbulent free convection. Ibl (21) presented a model to explain these results.

Several laboratory and micropilot scale experiments in two-phase flow with reactive gas have been reported. Examples include the production of H_2O_2 by O_2 reduction on graphite particles in fixed bed reactors (22) and the production of oxalic acid from CO_2 in a parallel-plate reactor (23). However, these studies concentrated on problems related to current efficiency and cell voltage and did not address fundamental mass-transport processes.

In summary, transport literature exists for a wide variety of multiphase processes involving gas-liquid-solid systems, but there are no known works on transport to a solid reactive surface exposed to two-phase flow in which the gas phase contains the reactant. This type of system, however, is encountered in the electrolysis of gaseous feedstocks. The present study was therefore carried out to improve fundamental understanding of the sequence of events which occurs and to establish correlations for multiphase transport processes in channel electrolyzers.

Apparatus

The parallel-plate electrolyzer was similar to that used previously by Lu (2) and consisted of a divided cell having two flow circuits as illustrated schematically in Fig. 1. The cell was machined from two polypropylene blocks. Working electrodes of DSA® (2.7 × 27 cm exposed, Diamond Shamrock Corporation) or of Pt (2.7 × 26 cm, pressed against a 316 SS sheet) were used. Adjacent to and coplanar with the working electrode were two additional electrodes made of DSA® (2.7 × 10 cm) which served to eliminate entrance and exit effects; of these electrodes, the downstream electrode was used as the reference electrode for the ferricyanide reduction experiments. The counterelectrode was made of porous DSA® (3.1 × 27 cm, Diamond Shamrock Corporation) and was positioned so that electrolyte flowed through the pores toward the working electrode compartment (Fig. 1). Electrical contact to electrodes was made by titanium screws pressed onto the back side of the electrodes and was found to have a contact resistance of less than 0.1Ω.

A microporous polypropylene separator (Daramic, W.R. Grace & Company) was used to prevent bulk flow between the anolyte and catholyte compartments. The separator had support ribs in the direction of flow to avoid buckling and was held at a distance of 0.2 cm from each electrode surface. On the working electrode side, there
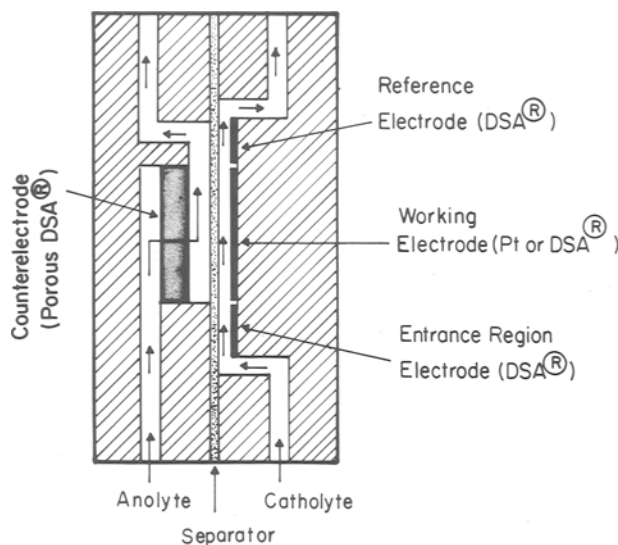
Fig. 1. Schematic of the flow circuits inside the cell (not drawn to scale). Reference electrode shown was used for the ferricyanide reduction experiments.
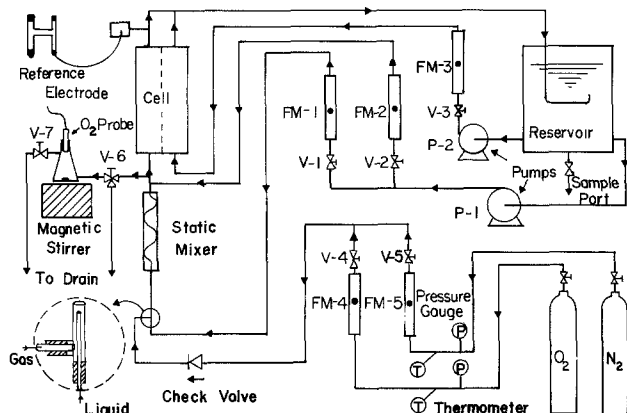
Fig. 2. Schematic of the flow system. Oxygen measuring system and reference electrode used for the oxygen-reduction experiments are included.

were three ribs dividing the catholyte chamber into two identical channels, each with cross-sectional dimensions of 1.35 × 0.2 cm. While in operation, the cell was positioned vertically.

Flow-visualization experiments were performed by replacing the separator and polypropylene counterelectrode block by a transparent Plexiglas sheet, of which the surface facing the working electrode was machined to exactly simulate the separator geometry.

The flow circuit illustrated in Fig. 2 consisted of delivery lines for gas and liquid streams which were combined in a Static Mixer® and passed to the working electrode compartment of the cell. Pump P-1 (March, no. TE-MDX-MT-3) fed the Static Mixer® with liquid electrolyte taken from the reservoir (4 liter capacity) at a rate controlled by valve V-1 and measured by meter FM-1 (Gilmont no. 4, Ti float). A second liquid metering system, V-2 and FM-2, was used to augment the flow from the Static Mixer® in order to achieve a wider range of variables. There were two gas-delivery systems containing calibrated flowmeters FM-4 (Gilmont no. 1, glass float) and FM-5 (Gilmont no. 2, glass float). Either or both systems could be used to control delivery rate of a single gas or of a gas mixture of known composition. The pressure of the gas was kept at 7 psig, determined by pressure gauges Ⓟ, while the gas temperature was measured with thermometers Ⓣ. The pressure in the cell was essentially 1 atm absolute.

The Static Mixer® (Kenics) used to generate a homogeneous dispersion of bubbles had a 3/16 in. id with 20 elements of 316 SS in a housing of the same material. The mean bubble size was measured from pictures of the two-phase mixture flowing through the working electrode compartment.

Pump P-2 (March, no. TE-MDX-MT-3) fed the counterelectrode compartment through flowmeter FM-3 (Gilmont no. 4, Ti float). After passing through the cell, the anolyte and catholyte streams merged and returned to the reservoir, where the gas was vented to the atmosphere and the liquid was recirculated. Anode and cathode reactions of ferri and ferrocyanide exhibited 100% c.e., so

there was no net concentration change in the recirculating system.

In experiments which involved oxygen reduction, the concentration of oxygen was measured just before the cell entrance with use of a calibrated dissolved-O_2 probe (Lazar, no. DO-166) in connection with the mV scale of a pH meter (Metrohm/Brinkmann pH-104). The O_2 concentration thus obtained was accurate to within ±0.2 ppm.

Power to the cell was provided by a potentiostatic supply (Wenking, no. 70TS1) controlled by a function generator (PAR, no. 175). A cathodic-potential ramp was used to measure the limiting current plateau, which was displayed on an X-Y recorder (Houston, no. 2000).

Procedures

Table I lists the experimental systems that were used in this study. All solutions were prepared by mixing analytical-grade reagents with deionized, distilled water (conductivity $<3 \times 10^{-6}$ $(\Omega\text{-cm})^{-1}$). For the ferricyanide-reduction experiments, equimolar solutions of the redox couple were used in concentrations which ranged between 1 and 10 mM, as determined by iodometric titration (25).

The physical properties of the electrolyte solutions and the transport properties of the electrochemical reactants were measured and compiled in Table II. The density was measured by weighing a known solution volume, while the viscosity was found with an Ostwald viscometer. Diffusivities were determined with a Pt RDE (Pine, no. ASR, 366).

In order to obtain reproducible results, the Pt electrode was washed in acetone and distilled water, immersed in a chromic-sulfuric acid cleaning solution for 20 min, rinsed thoroughly, placed in the cell and activated in supporting electrolyte by sweeping five times between -1.2 and 0.8V vs. Hg/HgO (0.5M KOH), and then set at -1.2V vs. Hg/HgO for 2 min to reduce surface oxides. The DSA® electrode was degreased in trichloroethylene and rinsed with acetone and then water before being placed in the cell. No activation was necessary. The DSA® electrode was used for ferricyanide-reduction experiments only.

All electrolyses were carried out at about 25°C. For one-phase experiments with ferricyanide, the flow system was rinsed with distilled water and refilled with supporting electrolyte. An aliquot of stock solution containing reactant was then added, and the resulting solution was deaerated for 1h prior to use. The voltage scan was carried out at 5 mV/s. After completion of experiments at a given reactant concentration, an additional ali-

Table II. Physical and transport properties of the solutions used (at 25°C)

	0.2M Na$_2$SO$_4$	0.1M Na$_2$SO$_4$ + 0.2M KOH
Density (g/cm³)	1.05	1.02
Kinematic viscosity (cm²/s)	9.45 10^{-3}	9.28 10^{-3}
Ferricyanide diffusivity (cm²/s)	0.65 10^{-5}	—
Oxygen diffusivity (cm²/s)	—	1.85 10^{-5}
Oxygen concentration in air-saturated solution (mM)	—	0.220
Sc number	1450	500

Table I. Experimental format for separating the mass-transfer mechanisms

Liquid phase	Gas phase	Mechanism contributing to the current measured	Working-electrode reaction
Ferri/ferrocyanide in 0.2M Na$_2$SO$_4$	—	One-phase convective flow mechanism	$Fe(CN)_6^{3-} + e \rightarrow Fe(CN)_6^{4-}$
Air-saturated 0.2M KOH	—	One-phase convective flow mechanism	$O_2 + 2H_2O + 4e \rightarrow 4\,OH^-$
Ferri/ferrocyanide in 0.2M Na$_2$SO$_4$	N$_2$	One-phase convective flow + disturbance mechanism	$Fe(CN)_6^{3-} + e \rightarrow Fe(CN)_6^{4-}$
Saturated solution of 0.2M KOH + 0.1M Na$_2$SO$_4$	O$_2$ - N$_2$ mixtures	One-phase convective flow + disturbance + extraction mechanism	$O_2 + 2H_2O + 4e \rightarrow 4\,OH^-$

quot of stock solution containing reactant was added to increase the concentration to a new level, and the procedure was repeated.

For two-phase ferricyanide-inert gas experiments, the procedure was identical, except than N_2 gas was metered into the Static Mixer®, and the scan rate was 10 mV/s. Limiting currents were measured in sequence of experiments, each at constant liquid flow rate with successively increasing gas flow rates.

For one-phase experiments with dissolved oxygen as the reactant, the electrolyte was circulated through the flow system for 30 min while air was sparged into the reservoir. The Pt electrode was then activated, the O_2 concentration was measured with the dissolved oxygen probe, and current-potential curves were recorded at a scan rate of 5 mV/s. A Hg/HgO (0.5M KOH) reference electrode (built in-house) was used for all the experiments involving the O_2 reduction reaction.

For two-phase experiments with reactive gas bubbles, air, or other N_2-O_2 mixtures (depending on the desired O_2 concentration) were dispersed in the electrolyte phase. The procedure was similar to that followed for the two-phase inert-gas experiments, except that special care was taken to ensure that the Pt electrode remained active. The electrode was periodically reactivated, and the gas was periodically shut off and a one-phase experiment was carried out to confirm reproducibility of the Pt surface. Repeated experiments were reproducible to within 3% for one-phase flow and to within 12% for two-phase flow with reactive gas. Two-phase inert-gas experiments were reproducible to within 5%.

Results

Flow visualization.—Flow-visualization experiments indicated several types of flow patterns, depending upon the flow rates of the two phases, as shown in Fig. 3. In the bubbly-flow regime, the gas was uniformly distributed as a swarm of tiny bubbles. In the slug-flow regime, some gas was in large bullet-shaped bubbles which almost spanned the interelectrode gap; these large bubbles were separated by slugs of liquid containing tiny gas bubbles. In the region of low liquid flow rates, the flow patterns were not reproducible; this nonreproducible region was avoided in the measurement of mass-transfer coefficients.

It was found that the electrolyte composition had a strong influence on bubble coalescence. For example, the bubbles formed in 0.2M Na_2SO_4 were extremely fine in comparison with those formed, under otherwise iden-
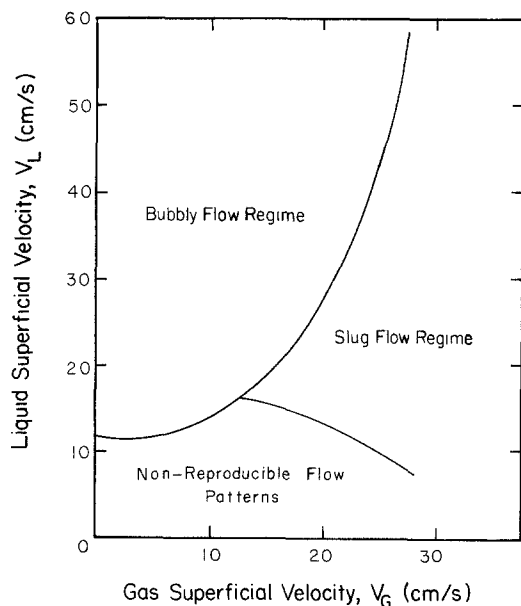
tical conditions, in distilled water or in 0.2M H_2SO_4. It was further found that the mixed electrolyte solution (0.2M KOH + 0.1M Na_2SO_4) used for two-phase oxygen-reduction experiments displayed the same behavior, with respect to bubble sizes, as the 0.2M Na_2SO_4 solution used for the two-phase ferricyanide-reduction experiments.

Analysis of limiting current data.—The one-phase mass-transfer coefficient, k_o, was obtained from cathodic limiting current measurements on solutions having known concentrations of reactant, ferricyanide, or oxygen, as shown in Table I

$$k_o = \frac{i_o}{nFc_{bL}} \qquad [2]$$

Under the conditions investigated, the O_2 reduction reaction proceeded by a 4-electron pathway. The two-phase disturbance-mechanism coefficient, k_d, was found from limiting current data obtained with ferricyanide solutions containing dispersed N_2; by subtracting the limiting current owing to the one-phase convective flow as found previously for the same liquid flow rate, the current attributable to the disturbance mechanism was obtained

$$k_d = \frac{(i_o + i_d)}{nFc_{bL}} - k_o \qquad [3]$$

As indicated in Table I, the two-phase extraction-mechanism coefficient, k_e, was found by dispersing air (or other O_2-N_2 mixtures) in a solution of mixed KOH-Na_2SO_4 electrolyte. The limiting current thus measured was due to all three mechanisms. After subtracting the limiting current measured under the same hydrodynamic conditions, with N_2 dispersed in ferricyanide solution (corrected for differences in diffusivity, concentration, and n value), the extraction-mechanism mass-transfer coefficient could be obtained

$$k_e H = \frac{(i_o + i_d + i_e)}{nFc_{bL}} - (k_o + k_d) \qquad [4]$$

Equation [4] is obtained after manipulating Eq. [1], assuming that the equilibrium between gas- and liquid-phase compositions can be described for the O_2 system by Henry's law, $c_{bG} = Hc_{bL}$.

One-phase convective flow mechanism.—The theoretical average limiting current density for mass transfer in laminar flow between infinite parallel plates is (4)

$$i_o = 1.85 \frac{nFDc_{bL}}{s} \left[\frac{V_L}{dDL} \right]^{1/3} \qquad [5]$$

where $d = 2h$. However, as verified by Pickett and Stanmore (26), the same equation can also be used for channels with finite dimensions, provided that the hydraulic diameter of the duct replaces the equivalent diameter, i.e., $d = 2Wh/(W + h)$. Figure 4 indicates that data for both the ferricyanide and the dissolved oxygen electrode were in good agreement with Eq. [5] for Reynolds numbers up to 2100 (55 cm/s), where transition to turbulent flow sets in (4). A further consequence of Eq. [5] is that a graph of $i_o/V_L^{1/3}$ vs. c_{bL} should give a straight line through the origin. This relation was verified for ferricyanide reduction on both DSA® and Pt electrodes over the range of 1-10 mM.

The mass-transfer coefficient for one-phase flow is therefore

$$k_o = \frac{1.85D}{s} \left[\frac{V_L}{dDL} \right]^{1/3} \qquad [6]$$

and can be used to estimate the diffusion-layer thickness, $\delta = D/k_o$. At the highest flow rate, the diffusion-layer thickness (50 μm) was ten times larger than the DSA® electrode-surface roughness (5 μm), so the electrode may be characterized as "smooth" for the one-phase ex-

Fig. 3. Flow-pattern map for N_2-0.2M Na_2SO_4 two-phase flow through the working electrode compartment.
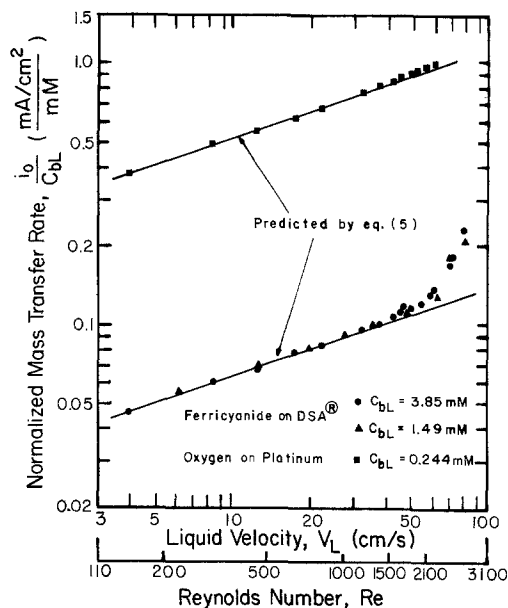
Fig. 4. Normalized mass-transfer rate vs. liquid velocity in one-phase flow. Re refers to the ferricyanide-0.2M Na_2SO_4 solution Reynolds number.

Fig. 5. Mass-transfer rate in two-phase flow with inert (N_2) gas vs. ferricyanide concentration in bulk solution.

periments. The shiny Pt electrode was essentially "smooth" for the one- and two-phase experiments.

The effect of a turbulence promoter (VEXAR 549V300, du Pont) was to increase the mass-transfer coefficient. In the range $6 < V_L < 60$ (cm/s), the mass-transfer limiting current density followed the correlation

$$i_o = 0.0177 \ V_L^{0.70} c_{bL} \qquad [7]$$

The exponent on velocity (0.70) is larger than in Eq. [5] and is indicative of the increased stirring effect. Over the range investigated, the limiting current was increased as much as threefold by the presence of the turbulence promoter.

Two-phase disturbance mechanism.—Because the gas bubbles rise with respect to the liquid during transit through the electrolyzer, they impart a transverse momentum to the surrounding fluid which is absent in single-phase laminar flow and which influences the mass-transfer processes near the electrode surface. Additional sources of mixing action would include sudden motions imparted during bubble coalescence and/or breakup in the shear region near the electrode surface, as well as agitation in the wake region behind rising bubbles. For these reasons, the mass-transfer enhancement by the disturbance mechanism cannot be solely attributed to decreased channel cross-sectional area available for liquid flow and to consequentially increased liquid velocity. This situation is especially true for the narrow channel used in this work (0.2 cm channel gap).

For the case of two-phase flow with inert gas, Eq. [1] is simplified ($c_{bc} = 0$) to

$$i_o + i_d = nF \ (k_o + k_d) \ c_{bL} \qquad [8]$$

where the left-hand side represents the experimentally measured current density, k_o is given by Eq. [6], and c_{bL} was measured experimentally. Figure 5 illustrates that the form of Eq. [8] correctly correlates the mass-transfer behavior of the disturbance mechanism, in that data fall upon straight lines which pass through the origin and exhibit slopes that depend upon liquid- and gas-flow velocities.

Figure 6 illustrates how the mass-transfer rate due to both the one-phase convective flow mechanism and the disturbance mechanism varies with gas superficial velocity for several values of liquid superficial velocity. The superficial velocities of both phases were calculated by dividing the corresponding flow rate (that for the gas at 25°C and 1 atm) by the channel cross-sectional area. The
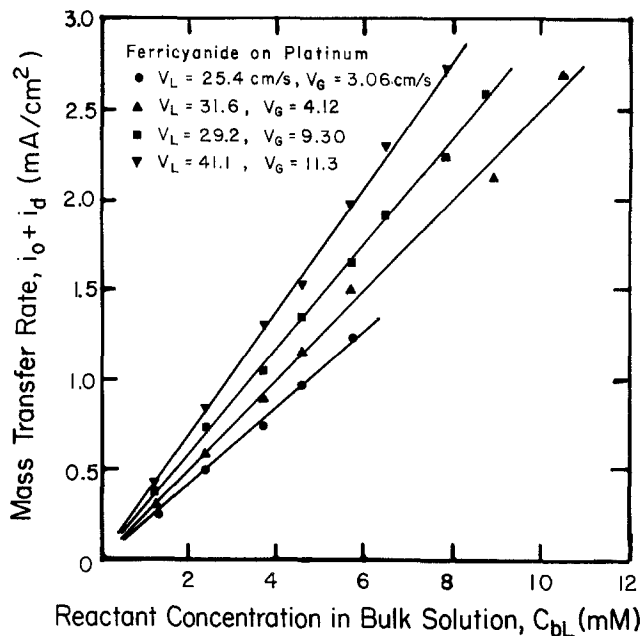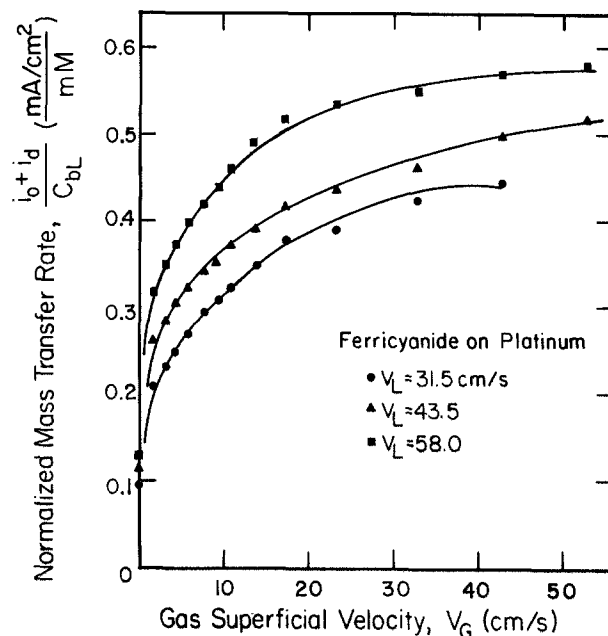

Fig. 6. Normalized mass-transfer rate in two-phase flow vs. nitrogen superficial velocity with the liquid superficial velocity as a parameter.

points on the $V_G = 0$ axis correspond to one-phase flow data. A substantial increase in the mass-transfer rate is obtained even when the gas flow rate is very small. For example, the limiting current is essentially doubled by gas velocities which are only 5% of the liquid velocity. This suggests that increased mass-transfer rates can be achieved for low gas-void fractions for which solution resistivity and pressure drop do not differ appreciably from the one-phase flow values.

Figure 6 also illustrates that the mass-transfer coefficient increases to a limiting value. For high gas velocities, a flow transition occurs from bubbly to slug flow, as indicated previously in Fig. 3. It is known (27) that slug flow is not as effective as bubbly flow in enhancing mass transport. A similar leveling of the transport rate in bubble columns has been reported by Ibl *et al.* (18), Novosad (27), Mersmann (10), and Steiff and Weinspach (11).

Figure 6 further shows that, for a given gas velocity, the mass-transfer coefficient increases with increasing liquid

velocity, a result which is in contrast to that reported by Sigrist *et al.* (20). However, in their experimental system, the interelectrode gap was at least five times wider than that used here, and, additionally, the liquid velocity employed was too low to be used in the present system while remaining in the bubbly flow regime. The explanation of these data by Ibl (21) was based on turbulent natural-convection concepts. Sigrist *et al.* realized that a decrease in the mass transfer with increasing liquid velocity (at constant gas velocity) would be observed provided that the liquid velocity is not too large. In studies of heat transfer in two-phase flow, others have reported conditions where the heat-transfer coefficient increases with liquid velocity (28) at high gas flow rates and where the coefficient is insensitive to liquid velocity (11) at low liquid flow rates. Thus it may be concluded that the disturbance effect is complex and that it depends upon the particular flow regime of operation. In the present work, the liquid velocity is appreciably higher than considered previously (20, 21), so explanations of behavior cannot be based on natural-convection phenomena.

Figure 6 also demonstrates that the disturbance mechanism can enhance the one-phase mass-transfer rate by up to 400%. Similarly, large enhancement factors have been reported elsewhere (11). In contrast, in studies on two-phase liquid-liquid systems, Lu and Alkire (2) reported an increase of up to 170%. The substantially greater enhancement in gas-liquid systems results from the significantly greater bubble-rise velocities in comparison with liquid droplets, owing to a greater density difference.

When the data in Fig. 6 are replotted on log-log coordinates, a slope of approximately 0.25 is found, which compares favorably to experimental and theoretical results reported for bubble columns (12).

After subtracting the contribution of the one-phase convective flow, the enhancement of mass transfer by the disturbance mechanism was found to be expressed by the empirical correlation

$$i_d = 0.007 \ V_L^{0.74} V_G^{0.36} c_{bL} \qquad [9]$$

which describes the data, for the bubbly-flow regime, to within 8%.

For the two-phase inert-gas experiments, the DSA® electrode gave currents which were about 10% higher than on the Pt electrode. Because the two-phase mass-transfer boundary layer can be as thin as 10 μm, this effect was attributed to the roughness of the DSA® material (about 5 μm), while the shiny Pt was essentially smooth.

By using two different Static Mixers®, it was possible to vary the mean bubble diameter by a factor of two. For the 3/16 in. unit, the diameter ranged between 200 and 600 μm, and for a 1/4 in. unit, the diameter ranged between 400 and 1200 μm. The effect of bubble size upon the mass-transfer rate was smaller than 5%. Others have reported similar observations in both gas-liquid (18, 29) and liquid-liquid systems (2).

When a turbulence promoter was placed in the flow channel, the influence upon two-phase inert-gas mass transfer was negligible. These results suggest that the two-phase mixture was by its nature "well mixed" and that the turbulence promoter provided little additional mixing. While the promoter might be expected to alter the mean bubble size, the results of the previous paragraph indicate that the mass-transfer enhancement is insensitive to bubble size.

Two-phase extraction mechanism.—When an electrochemically reactive gas is introduced as the second phase, a further mass-transfer enhancement occurs, as is depicted in the upper portion of Fig. 7. The gas-side mass-transfer resistance is negligible (30), so the oxygen concentration at the gas-liquid bubble interface is at the saturation concentration. Furthermore, the solution far from the electrode is saturated in oxygen as well. However, a bubble may penetrate the mass-transfer boundary layer near the electrode surface and may provide, by extraction of oxygen from the bubble, an increase in local oxygen
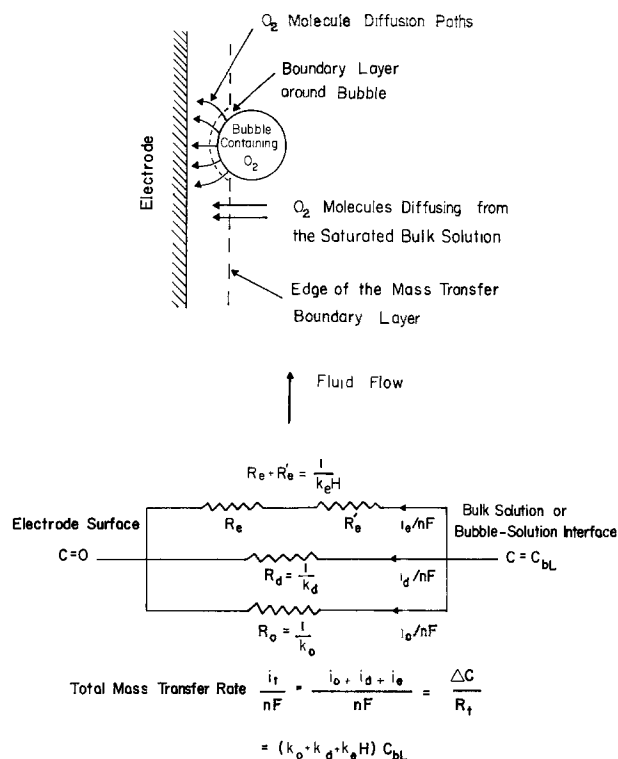

Fig. 7. (top) Mass-transfer mechanism in two-phase flow with reactive gas. (bottom) Equivalent resistive network.

concentration which would enhance the overall mass-transfer rate above that experienced by the disturbance mechanism of unreactive bubbles. It is to be expected that attachment of gas bubbles to the electrode is unlikely to occur at the polar electrode materials used in this study, so there will always be a liquid film separating the bubbles from the electrode. The lower portion of Fig. 7 indicates an equivalent resistive network describing the mass-transfer processes which are operative in the case of two-phase reactive-gas experiments. The extraction mechanism has been represented by two resistors in series, one of which (R'_e) accounts for the gas-to-liquid interfacial resistance, the other (R_e) for the further transport of the reactant to the electrode surface.

With use of Henry's law, Eq. [1] becomes

$$i_t = i_o + i_d + i_e = n\mathbf{F} \ (k_o + k_d + k_e H) \ c_{bl} \qquad [10]$$

For the conditions investigated in this study, the Henry's law constant for oxygen, $H = c_{bc}/c_{bL}$, had a value of 39. Data in Fig. 8 verify that the proposed additive correlation is appropriate. The variation in intercept may be attributed to drift in the "zero" of the oxygen probe and to uncertainty (at a level of 6.25×10^{-3} mM) in measurement of dissolved oxygen concentration by the probe. The data which follow were obtained at oxygen-saturation concentrations of 0.220 mM, for which probe errors were less than 8%.

The dependence of the measured total limiting current density on air superficial velocity is shown in Fig. 9 for three liquid superficial velocities. It is remarkable that for a given liquid velocity, the overall mass-transfer coefficient can be increased over the one-phase value by almost one order of magnitude by introduction of reactive gas. Indeed, the limiting current can be increased over the one-phase value by a factor of 7 with only 10% gas-volume ratio. The data shown in Fig. 9 exhibit similar behavior to the two-phase inert-gas data (Fig. 6) and, for the bubbly-flow regime, can be correlated by the empirical expression

$$i_t = 0.40 \ V_L^{0.60} V_G^{0.23} c_{bl} \qquad [11]$$

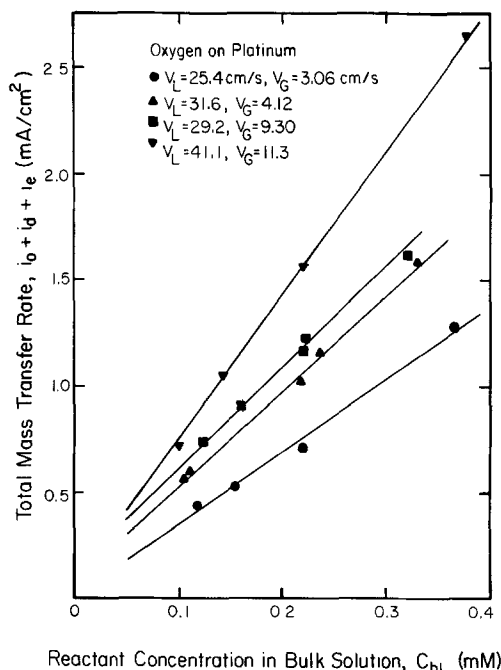which is good for $V_G > 1.8$ cm/s and describes the data to within 10%.

Fig. 8. Total mass-transfer rate in two-phase flow with reactive (O_2) gas vs. dissolved-oxygen concentration in bulk solution.
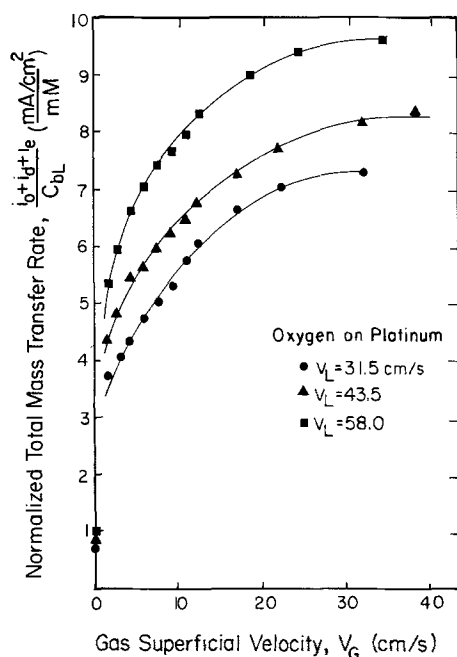

Fig. 9. Normalized mass-transfer rate in two-phase flow vs. air superficial velocity with the liquid superficial velocity as a parameter.

The relative importance of the extraction mechanism was found to be as follows

$$k_e H = (1.19 \pm 0.10)(k_o + k_d) \qquad [12]$$

One intuitively expects that larger values of $(k_o + k_d)$ correspond to smaller bubble-electrode distances and, therefore, larger k_e. However, the linear relationship between i_e and $(i_o + i_d)$ implied by Eq. [12] may not be true in cases where, owing to high conversion of the reactant, replenishment of the bulk solution by the reactive bubbles occurs in addition to replenishment of the mass-transfer boundary layer.

Variation of bubble size, created with use of two different Static Mixers®, had no influence on mass-transfer rates in two-phase reactive-gas systems. This is in contrast to data obtained in two-phase liquid-liquid systems

with reactive droplets (2). The difference may be attributed to the wettability of the electrode used by the dispersed organic phase. Similarly, the presence of a turbulence promoter in the working electrode compartment did not contribute additional mass-transfer enhancement beyond that afforded by the two-phase reactive gas in the absence of the promoter.

Conclusions

The limiting current method was used to study the mass transfer to a solid electrode in cocurrent gas-liquid flow through a vertical parallel-plate cell. Both an inert gas and a reactive gas were investigated. Flow visualization experiments showed that for the flow rates of gas and liquid used, the cell was in either the bubbly-flow or slug-flow regime. The total mass-transfer rate was expressed as the sum of the contributions of three different mechanisms: (i) the one-phase convective flow mechanism associated with the liquid as if it were flowing alone through the cell; (ii) the disturbance mechanism associated with the presence of bubbles "disturbing" the boundary layer; and (iii) the extraction mechanism associated with the presence of reactive bubbles replenishing the mass-transfer boundary layer. An experimental format was developed which enabled the contribution of each of the mechanisms to the total mass-transfer rate to be measured separately and enabled the additive model to be verified. Operating variables investigated included gas and liquid flow rates, bubble size, and electrode material. In addition, the effect of placing a turbulence promoter in the channel was determined.

The experimental results support the following conclusions.

1. The one-phase flow results compared well with theoretical expectations.

2. The mass-transfer rate due to the disturbance mechanism, as well as the mass-transfer rate due to the extraction mechanism, was proportional to the reactant concentration in the bulk solution.

3. At a constant liquid superficial velocity, the mass-transfer rate due to both the one-phase convective flow mechanism and the disturbance mechanism (i) reached values up to five times larger than those corresponding to the same liquid velocity in one-phase flow, (ii) increased sharply with increasing gas superficial velocity at low gas velocities, (iii) approached a constant value at high gas velocities, (iv) was dependent on the gas superficial velocity to the 0.25 power, (v) was independent of the bubble size for bubbles with diameters in the range 200-1200 μm, (vi) did not change significantly when a turbulence promoter was placed in the channel, and (vii) was always higher on an electrode with rough surface (DSA®) when compared to the rate on a "smooth" electrode (Pt).

4. The mass-transfer rate due to the disturbance mechanism was dependent on the liquid superficial velocity to the 0.74 power and on the gas superficial velocity to the 0.36 power (for the bubbly-flow regime).

5. At a constant liquid superficial velocity, the total mass-transfer rate in two-phase flow with reactive gas (i) reached values one order of magnitude higher than those corresponding to the same liquid velocity in one-phase flow, (ii) increased dramatically with increasing gas superficial velocity at low gas velocities, (iii) approached a constant value at high gas velocities, (iv) was dependent on the gas superficial velocity to the 0.23 power (for the bubbly-flow regime), (v) was independent of the bubble size for bubbles with diameters in the range 200-1200 μm, and (vi) changed insignificantly when a turbulence promoter was placed in the channel.

6. For a given gas superficial velocity, the total mass-transfer rate in two-phase flow with reactive gas was dependent on the liquid superficial velocity to the 0.60 power (for the bubbly-flow regime).

7. The mass-transfer rate due to the extraction mechanism was proportional to the mass-transfer rate due to both the one-phase convective flow mechanism and the

disturbance mechanism, the proportionality factor being 1.19 ± 0.10.

The results of this study showed that the use of two-phase flow in electrochemical reactors incorporating a gas which is sparingly soluble in the liquid phase may be highly advantageous. In particular, high mass-transfer rates can be achieved at low gas-volume fractions. Thus, the solution resistivity and the pressure drop through the system do not differ significantly from the corresponding values in one-phase flow. Consider for example the case of a gas-void fraction $\epsilon = 10\%$. The conductivity of the solution (31) will be $\kappa = \kappa_0(1 - \epsilon)^{1.5} = 0.85\kappa_0$, and the energy consumption due to IR drop will increase by about 15%. Moreover, the pressure drop (32) will be

$$\frac{dP}{dx} = \left(\frac{1 + \epsilon}{1 - \epsilon}\right) \left(\frac{dP}{dx}\right)_L = 1.22 \left(\frac{dP}{dx}\right)_L$$

and the energy consumption for pumping will be 22% higher than that when operating in one-phase flow with the same liquid velocity. However, even at $\epsilon = 10\%$, the mass-transfer rate can be up to seven times that in one-phase flow (Fig. 9), which amounts to a 600% increase in productivity if the process is mass-transfer limited.

This work dealt with the case of negligible conversion per pass of the reactant through the cell. The enhancement due to the extraction mechanism was solely attributed to bubbles resaturating depleted regions within the mass-transfer boundary layer. In situations where the reactant conversion is high, however, the presence of the reactive bubbles resaturating the bulk solution as well will make the contribution of the extraction mechanism even more significant.

Acknowledgments

LIST OF SYMBOLS

c	reactant concentration, mM
d	equivalent diameter, cm
D	reactant diffusivity, cm^2/s
F	Faraday constant, 96,500 C/g-eq
h	gap of flow channel, cm
H	constant in Henry's law $(= c_{bt}/c_{bL})$
i	current density, mA/cm^2
k	mass-transfer coefficient, cm/s
L	electrode length, cm
n	number of electrons exchanged in electrode reaction
P	pressure, dyn/cm^2
R	equivalent mass-transfer resistance, s/cm
Re	Reynolds number in one-phase flow (dV_L/ν)
s	stoichiometric coefficient of reacting species
V	superficial velocity, cm/s
W	electrode width, cm

Greek Symbols

δ	diffusion-layer thickness, cm
ϵ	gas-void fraction
κ	solution conductivity, $(\Omega\text{-cm})^{-1}$
ν	solution kinematic viscosity, cm^2/s

Subscripts

b	bulk of gas or liquid phase
d	due to the disturbance mechanism
e	due to the extraction mechanism
G	gas phase
L	liquid phase
o	one-phase flow
t	total (all three mechanisms)

REFERENCES

1. D. Economou, M.S. Thesis, University of Illinois (1983).
2. P-Y. Lu and R. C. Alkire, *This Journal,* **131,** 1059 (1984).
3. R. W. Houghton and A. T. Kuhn, *J. Appl. Electrochem.,* **4,** 173 (1974).
4. J. Lee and J. R. Selman, *This Journal,* **129,** 1670 (1982).
5. J. Postlethwaite and D. N. Holdner, *Can. J. Chem. Eng.,* **54,** 255 (1976).
6. R. Dworak, H. Fees, and H. Wendt, *AIChE Symp. Ser.,* **75,** 38 (1979).
7. R. Dworak and H. Wendt, *Ber. Bunsenges. Phys. Chem.,* **81,** 728 (1977).
8. Y. T. Shah, B. G. Kelkar, S. P. Godbole, and W.-D. Deckwer, *AIChE J.,* **28 (3),** 353 (1982).
9. G. B. Wallis, "One-Dimensional Two-Phase Flow," McGraw-Hill, New York (1969).
10. A. Mersmann, *Chem-Ing.-Tech.,* **47,** 869 (1975).
11. A. Steiff and P.-M. Weinspach, *Ger. Chem. Eng.,* **1,** 150 (1978).
12. W.-D. Deckwer, *Chem. Eng. Sci.,* **35,** 1341 (1980).
13. H. Vogt, in "Comprehensive Treatise of Electrochemistry," Vol. 6, E. B. Yeager, J. O'M. Bockris, B. E. Conway, and S. Sarangapani, Editors, p. 445, Plenum Press, New York (1983).
14. T. R. Beck, *This Journal,* **116,** 1038 (1969).
15. H. Vogt, *Electrochim. Acta,* **23,** 203 (1978).
16. R. Alkire and P-Y. Lu, *This Journal,* **126,** 2118 (1979).
17. P-Y. Lu, Ph.D. Thesis, University of Illinois (1982).
18. N. Ibl, R. Kind, and E. Adam, *Anales De Quimica, 71,* 1008 (1975).
19. N. Ibl, *Chem-Ing.-Tech.,* **35,** 353 (1963).
20. L. Sigrist, O. Dossenbach, and N. Ibl, *J. Heat and Mass Transfer,* **22,** 1393 (1979).
21. N. Ibl, *Electrochim. Acta,* **24,** 1105 (1979).
22. C. Oloman and A. P. Watkinson, *Can. J. Chem. Eng.,* **54,** 312 (1976); U.S. Pat. 3,969,201 (1976) and 4,118,305 (1978).
23. J. Fischer, Th. Lehmann, and E. Heitz, *J. Appl. Electrochem.,* **11,** 743 (1981).
24. A. S. Gendron and V. A. Ettel, *Can. J. Chem. Eng.,* **53,** 36 (1975).
25. A. I. Vogel, "Quantitative Inorganic Analysis," 3rd ed., Longman, London (1961).
26. D. J. Pickett and B. R. Stanmore, *J. Appl. Electrochem.,* **2,** 151 (1972).
27. Z. Novosad, *Collect. Czech. Chem. Commun.,* **20,** 477 (1955).
28. S. R. Ravipudi and T. M. Godbold, *Heat Transfer 6th Int. Heat Transfer Conf.,* **1,** 505 (1978).
29. H. Kobel, W. Siemes, R. Mass, and K. Muller, *Chem-Ing.-Tech.,* **30,** 400 (1958)
30. M. Motarjemi and G. J. Jameson, *Chem. Eng. Sci.,* **33,** 1415 (1978).
31. D. A. G. Bruggemann, *Ann. Phys.,* **24,** 636 (1935).
32. H. Vogt, *J. Appl. Electrochem.,* **12,** 261 (1982).
33. J. R. Selman and C. W. Tobias, in "Advances in Chemical Engineering," Vol. 10, T. Drew, Editor, p. 211, Academic Press, New York (1978).
34. R. E. Acosta, R. H. Muller, and C. W. Tobias, *AIChE J.,* In press.